Available online at www.sciencedirect.com
ScienceDirect
Surface & Coatings Technology 201 (2006) 2419–2430
SURFACE & COATINGS TECHNOLOGY
www.elsevier.com/locate/surfcoat

Surface modification of resistance welding electrodes by electro-spark deposited composite coatings
Part II. Metallurgical behavior during welding

Zheng Chen [a,b,*], Y. Zhou [b]

[a] Department of Materials Science and Engineering, Jiangsu University of Science and Technology, Zhenjiang, 212003, PR China
[b] Department of Mechanical Engineering, University of Waterloo, 200 University Avenue West, Waterloo, Ontario, Canada, N2L 3G1

Received 21 October 2005; accepted in revised form 16 April 2006
Available online 5 June 2006

Abstract

Electrodes with monolithic TiC_P/Ni coatings and multi-layer Ni/(TiC_P/Ni)/Ni coatings were used to resistance spot weld Zn-coated sheet steel to investigate metallurgical behaviour of the coatings during welding. Scanning electron microscopy, energy-dispersive X-ray analysis and X-ray diffraction were employed to characterize the microstructure of coatings, reactions of electrodes with Zn-coating and alloy layer formation. The results showed that molten Zn penetrated TiC_P/Ni coatings via the cracks that were present within as-coated TiC_P/Ni coating, starting from the first weld. Additional cracks continually formed in the coating during welding due to action of the welding force on the low toughness coating, resulting in formation of a granular loose overlay at the outer surface which were easily detached and stuck onto the work sheet. On the contrary, cracks could be rarely found within Ni/(TiC_P/Ni)/Ni coating until 100 welds or more were made, and much fewer cracks formed up to 400 welds, compared to the TiC_P/Ni coating. With Ni/(TiC_P/Ni)/Ni coating on the electrode surface, alloying between copper alloy and molten Zn as well as pitting (erosion) of the electrode tips were remarkably reduced, and hence, a slower growth rate of tip diameter was observed.

Keywords: Resistance welding; Electrode; TiC; Ni; Composite; Coating; Zn-coated steel

1. Introduction

The use of zinc-coated steels has attracted much attention over the past decade owing to their good corrosion resistance and relatively low cost. Resistance spot welding is the primary method for joining sheet steel components in the automotive industries. However, the zinc coating has resulted in serious welding problems due to its lower electrical resistance and melting temperature, and accelerated degradation of resistance welding electrode tips. This leads to a drastic reduction in the electrode life. A short electrode life limits the rate of production due to the need for frequent electrode dressing and/or electrode changes. Electrode degradation during resistance welding of coated steels has been the subject of many studies, in which, for example, developments in electrode materials and design of electrode have been explored in an effort to improve weldability and increase electrode life [1–10]. It is commonly believed that Zn coatings will react with the electrodes to form brass alloys, causing electrode sticking due to local bonding between the electrode and workpiece. Fracture of these local bonds can lead to stripping of parts of the electrode surface causing progressive erosion and/or pitting which eventually causes growth of the tip diameter and, hence, the failure of the electrode.

On the other hand, coating the electrode surfaces has been suggested as a method by which to extend electrode life. For example, Dong and Zhou [11] have shown that an electrode with electro-spark deposited TiC_P/Ni composite coating can extend the life of micro-resistance welding electrodes. Their tests found the coating increases tip life by approximately 70% by reducing the amount of local bonding between electrode and Ni sheet. More recently, in addition, the use of the TiC_P/Ni

* Corresponding author. Tel.: +86 511 4401182.
E-mail address: chenz_31@yahoo.com.cn (Z. Chen).

0257-8972/$ - see front matter © 2006 Elsevier B.V. All rights reserved.
doi:10.1016/j.surfcoat.2006.04.010

Table 1
Welding parameters for testing of electrodes

	Welding current (A)	Electrode force (kN)	Weld time (cycle)	Hold time (cycle)	Welding rate (welds/min)	Cooling water (L/min)
Uncoated electrode	9200	1.94	11	5	25	2
Coated electrode	8500	1.94	11	5	25	2

composite coating for electrode life improvement in resistance spot welding of hot-dip galvanized zinc coated steel has also been reported and shown that TiC_P/Ni coating acts as a barrier against erosion and alloying of electrode by molten Zn [12]. The TiC_P/Ni composite coating, however, needs further improvement as a barrier layer due to the presence of cracks within the coating and delamination at the coating–substrate interface [13]. A modified coating approach has been described in Part I of the present work, where it was demonstrated that a dense and crack-free Ni/(TiC_P/Ni)/Ni coating could be deposited on electrode surfaces by a multi-layer electro-spark deposition process [13].

In the present work, the metallurgical behavior during resistance welding of Zn-coated steel using both monolithic TiC_P/Ni and multi-layer Ni/(TiC_P/Ni)/Ni deposited electrode coatings has been investigated.

2. Experimental

Electrodes were coated by electro-spark deposition either using TiC_P/Ni sintered composite rod (42 vol.% of TiC particle and 21 wt.% of Ni with addition of Mo and Co) to apply a monolithic TiC_P/Ni layer or using TiC_P/Ni and Ni rods to make a three-layer Ni/(TiC_P/Ni)/Ni coating, as described in Part I. The thickness of the coatings was around 35 μm. Welding tests of electrodes with and without coating were carried out using a 250 kV A single-phase AC spot welding machine. Hot dip galvanized (HDG60G) mild steel (0.7 mm thick with 0.01 mm thick Zn-coating on both side) was employed as worksheets. Welding test parameters used in this work are listed in Table 1 in order to investigate and compare the degradation process of electrodes with and without coating under same initial heat generation condition. As can be seen from Table 1, the welding current for coated electrodes was reduced to obtain a similar starting nugget diameter, which means that coated electrodes can generate the same heat at a lower current as that generated using uncoated electrodes at a higher current. Under such conditions, the growth rate of electrode tip diameter during welding was monitored as an evaluation parameter of electrode performance, determined by a carbon imprint technique in which a copy paper together with a carbon paper were put on the surface of a sheet steel to record the shape of electrodes top surface when electrodes contact with the sheet steel under pressure [12]. In order to investigate the metallurgical behavior of coatings during welding, after certain numbers of welds, tip surfaces and cross-sections of sacrificed electrodes, as well as worksheet weld surfaces were examined using a JEOL JSM-840 scanning electron microscope (SEM) equipped with energy-dispersive spectrometer (EDS). Phase identification was conducted using a Siemens D500 X-ray diffractometer (XRD) with Cu K_α radiation operating at 30 kV and 40 mA.

3. Results

3.1. Electrode tip growth during welding

Electrode tip growth has recently been suggested as the dominant process that determines electrode life when resistance spot welding Zn-coated steels [3]. It is also known that in terms of electrode wear rate, the change in the electrode tip diameter with increasing number of welds is more important than the absolute value of electrode face diameter itself [6]. Accordingly, the rate of tip diameter growth of electrodes without and with monolithic TiC_P/Ni coating or multi-layer deposited Ni/(TiC_P/Ni)/Ni coating during welding was first investigated in the present work. As shown in Fig. 1, the tip diameter growth rate of the electrode with monolithic TiC_P/Ni coating was similar to that of the electrode without coating before 100 welds. However, the former was much less than the latter when number of welds exceeded 100. On the contrary, the electrode with multi-Ni/(TiC_P/Ni)/Ni coating showed smaller tip diameter growth rate than that with monolithic TiC_P/Ni coating up to 400 welds.

3.2. XRD analyses

X-ray diffraction analysis was performed on the electrode tip surface before and after welding testing. Strong peaks of TiC were found from the X-ray diffraction pattern of electrode with as-deposited monolithic TiC_P/Ni coating, as shown in Fig. 2. After 400 welds, however, the intensity of TiC peaks significantly reduced, indicating loss of TiC_P/Ni coating during welding due to sticking and removal to the sheet. In addition, a

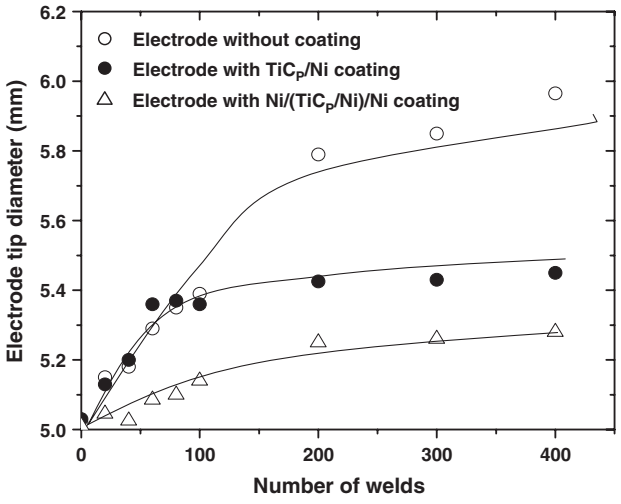

Fig. 1. Growth of electrode tip diameter as a function of weld number.

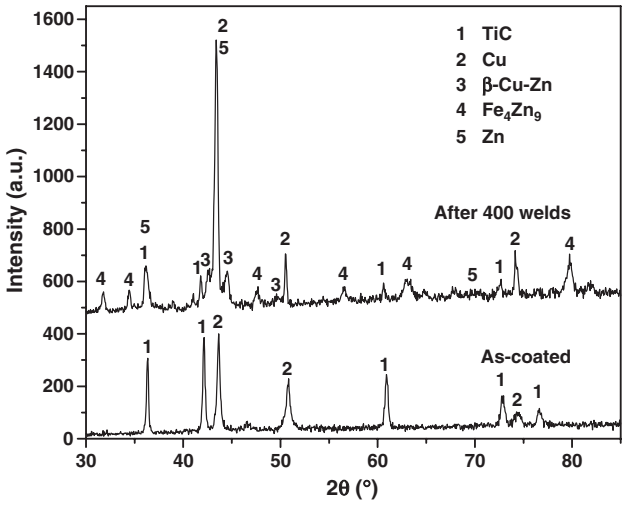

Fig. 2. XRD patterns taken from electrodes surface with monolithic TiC_P/Ni coating before welding (a) and after 400 welds (b).

β-Cu–Zn alloy was observed, resulting from the reaction between Zn and electrode copper alloy substrate. Fig. 3 exhibits the XRD patterns of the electrode with multi-layer Ni/(TiC_P/Ni)/Ni coating before and after 400 welds. Different from the monolithic TiC_P/Ni coating, the predominant phases of the as-deposited Ni/(TiC_P/Ni)/Ni coating were Ni and TiC. After 400 welds, the intensity of Ni remarkably decreased, indicating loss of the top Ni layer. However, Ni/(TiC_P/Ni) coating was still maintained on the electrode surface, as evidenced by strong TiC peaks. Moreover, there was no evidence that any reaction of the copper alloy substrate with the molten Zn had taken place. On the other hand, Zn and Fe–Zn compound were present on the electrode surfaces after welding.

3.3. SEM observation of monolithic TiC_P/Ni coating

Figs. 4 and 5 show surface photographs of an electrode with monolithic TiC_P/Ni coating after 1 weld, along with the EDX element maps of Ti, Cu, Fe and Zn. It is worth noting that only 1 weld sufficed to cause local loss (pitting) of TiC_P/Ni coating (Fig. 4) and penetration of molten Zn via cracks into the coating (Fig. 5). Fig. 6 illustrates a low-magnification surface photograph of an electrode with monolithic TiC_P/Ni coating after 100 welds. It can be clearly seen from Fig. 6 that much TiC_P/Ni coating had been removed, allowing molten Zn and/or Zn–Fe to directly react with Cu to form brass alloys. The high-magnification SEM photographs of the electrode surface after 100 welds demonstrated that the initial cracks within the TiC_P/Ni coating had been sealed by penetrated and solidified Zn containing Fe (Fig. 7). The sealing of cracks in the TiC_P/Ni coating was similar to a brazing process that might prevent TiC_P/Ni coating from removal due to sticking. On the other hand, comparing the diameter of islands within as-deposited TiC_P/Ni coating (~250 μm), the most important finding was that the diameter of islands reduced to 50–80 μm after 100 welds, indicating ongoing cracking of the coating due to its low toughness and action of welding force upon each weld event. When welding was continued to 400 welds, the diameter of uncracked islands decreased to 30–60 μm, and cracks were again found between sealed Zn–Fe alloy and TiC_P/Ni coating, as shown in Fig. 8.

Fig. 9 shows the cross-section of an electrode with TiC_P/Ni coating after 100 welds. The average thickness of TiC_P/Ni coating decreased to about 20 μm from its original thickness (approximately 35 μm). It is interesting to note that the TiC_P/Ni coating could be divided into two different regions. (i) The region close to the outer surface marked by "A" was granular and loose in which some cracks had been formed. (ii) The region adjacent to copper alloy substrate marked by "B" was relatively dense as compared with region "A." But some grooves that had been sealed by Zn–Fe alloy existed within the region "B." In addition, Fig. 9 clearly shows that Zn mainly penetrated through the cracks formed in the granular TiC_P/Ni layer and the grooves in the dense layer to react with copper to form a 12-μm-thick Cu–Zn alloy layer underneath the TiC_P/Ni coating (layer "C" in Fig. 9). Fig. 10 illustrates the cross-section of an electrode with TiC_P/Ni coating after 400 welds. The integrated and dense TiC_P/Ni coating was no longer present, leaving non-continuous and separate loose TiC_P/Ni coating islands on the surface of the substrate. The thickness of Cu–Zn alloy layer increased to 30 μm, and cracks had formed within Cu–Zn alloy layer due to its brittleness.

3.4. Metallurgical phenomena of multi-layer deposited Ni/(TiC_P/Ni)/Ni coating

The surface photographs of electrode with multi-Ni/(TiC_P/Ni)/Ni coating after 1 weld are shown in Fig. 11, along with the EDX element maps of Ti, Ni and Zn. Comparing to Figs. 4 and 5, Zn was found randomly deposited on the surface of multi-Ni/(TiC_P/Ni)/Ni coating, no penetration of molten Zn into the coating could be seen owing to the absence of cracks within the coating. After 10 welds, the multi-Ni/(TiC_P/Ni)/Ni coating was still dense and did not show any cracking. However, cracks were detected within the Ni/(TiC_P/Ni)/Ni coating after welding

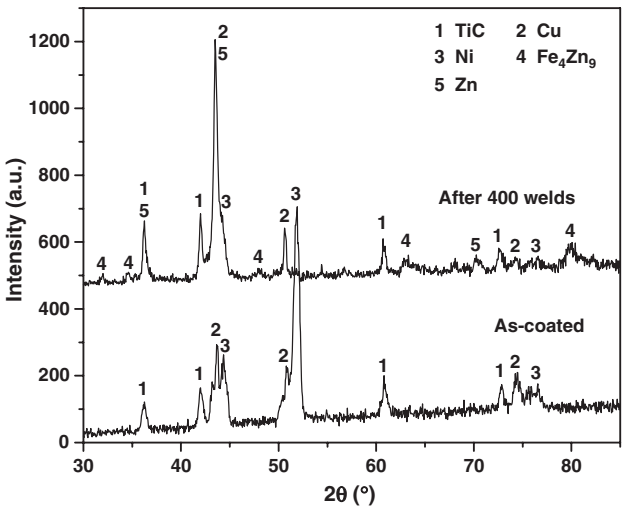

Fig. 3. XRD patterns taken from electrodes surface with multi-layer Ni/(TiC_P/Ni)/Ni coating before welding (a) and after 400 welds (b).

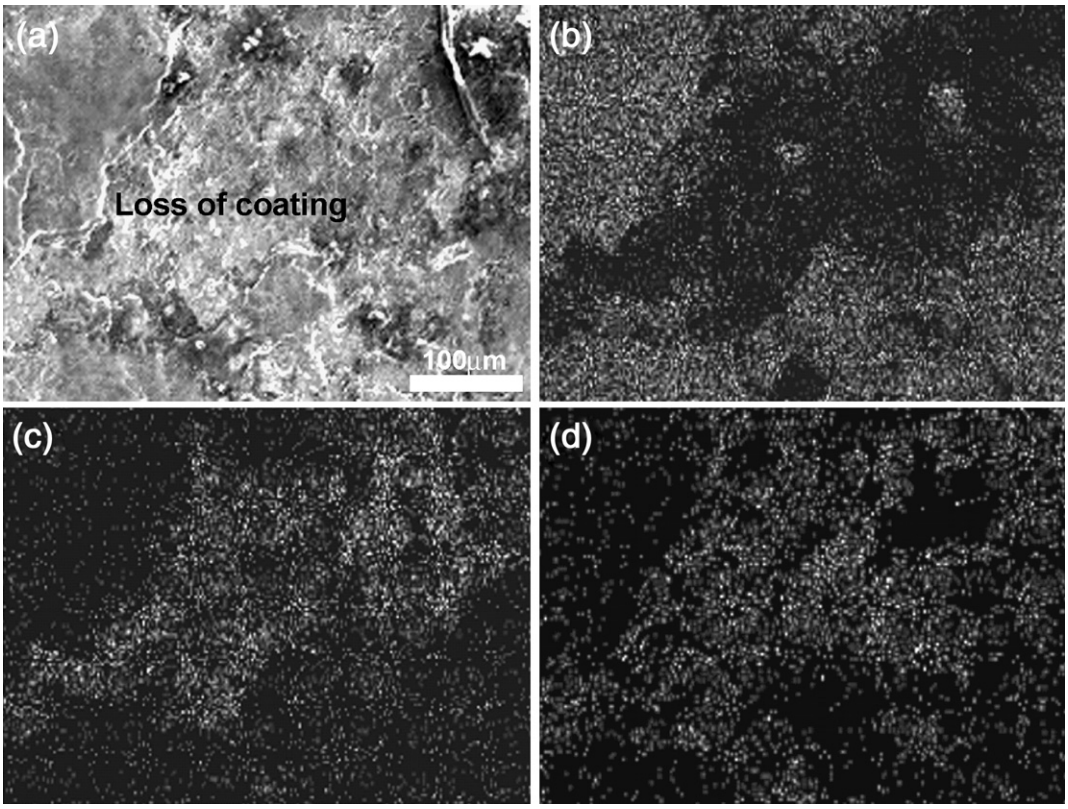

Fig. 4. SEM surface image of electrode with TiC_P/Ni coating after 1 weld showing loss of coating (a) and corresponding EDX element maps of Ti K_α (b), Cu K_α (c) and Zn K_α (d).

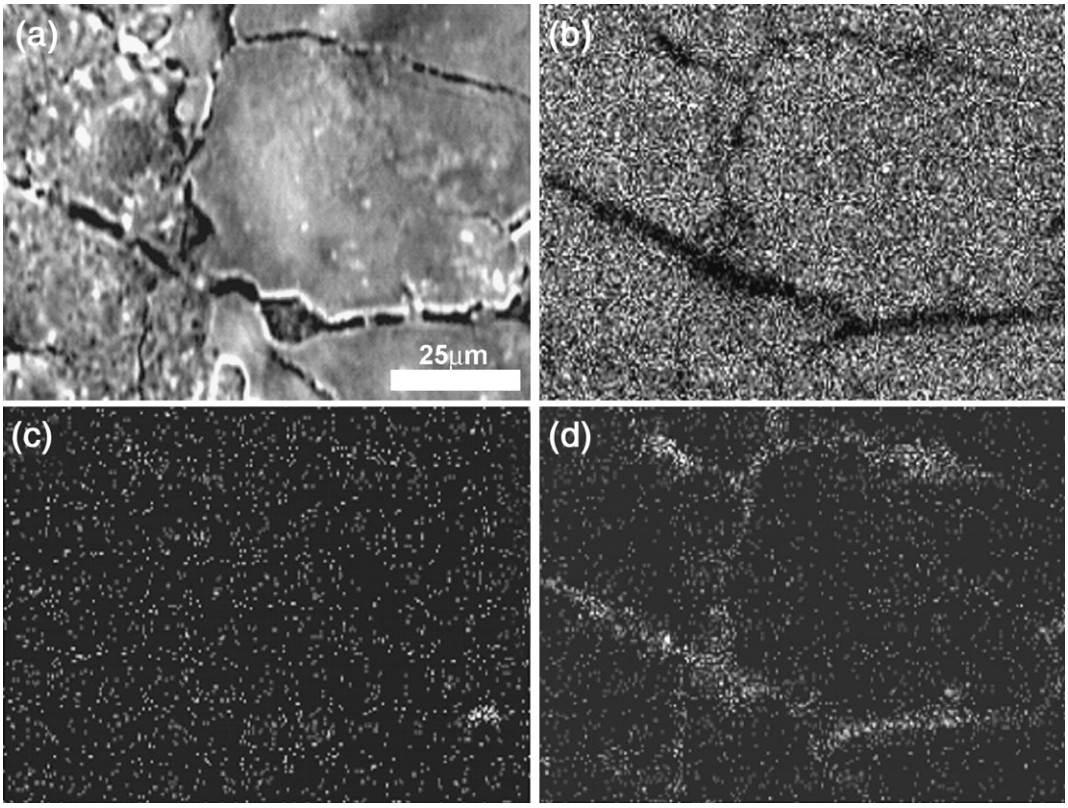

Fig. 5. SEM surface image of electrode with TiC_P/Ni coating after 1 weld showing penetration of molten Zn containing Fe (a) and corresponding EDX element maps of Ti K_α (b), Fe K_α (c) and Zn K_α (d).

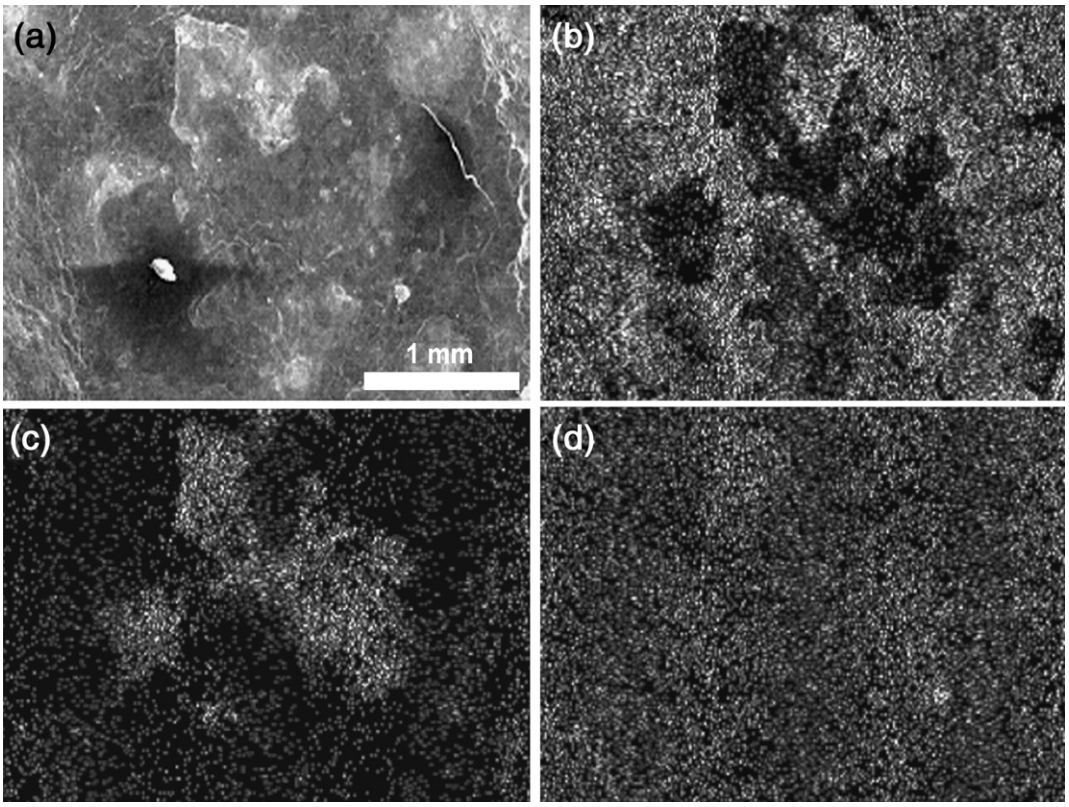

Fig. 6. Low-magnification SEM surface image of electrode with TiC_P/Ni coating after 100 welds showing removal of coating (a) and corresponding EDX element maps of Ti K_α (b), Cu K_α (c) and Zn K_α (d).

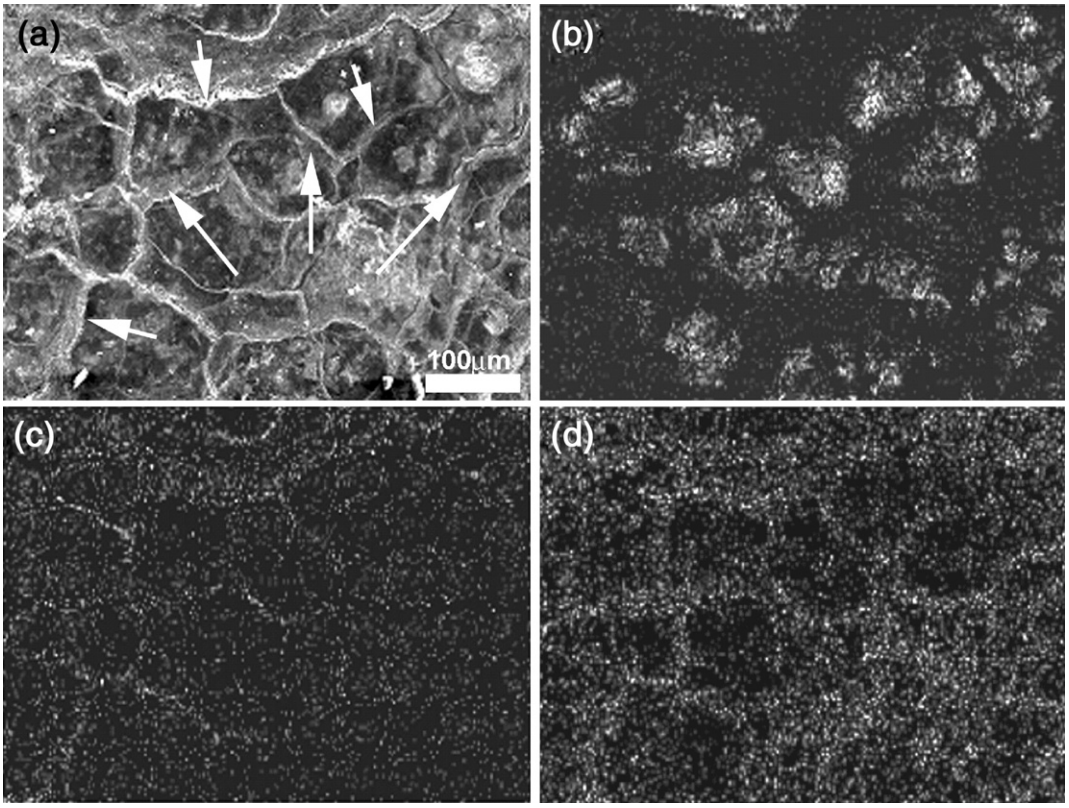

Fig. 7. High-magnification SEM surface image of electrode with TiC_P/Ni coating after 100 welds (a) showing sealing of cracked coating by penetrated Zn–Fe (indicated by arrows) and corresponding EDX element maps of Ti K_α (b), Fe K_α (c) and Zn K_α (d).

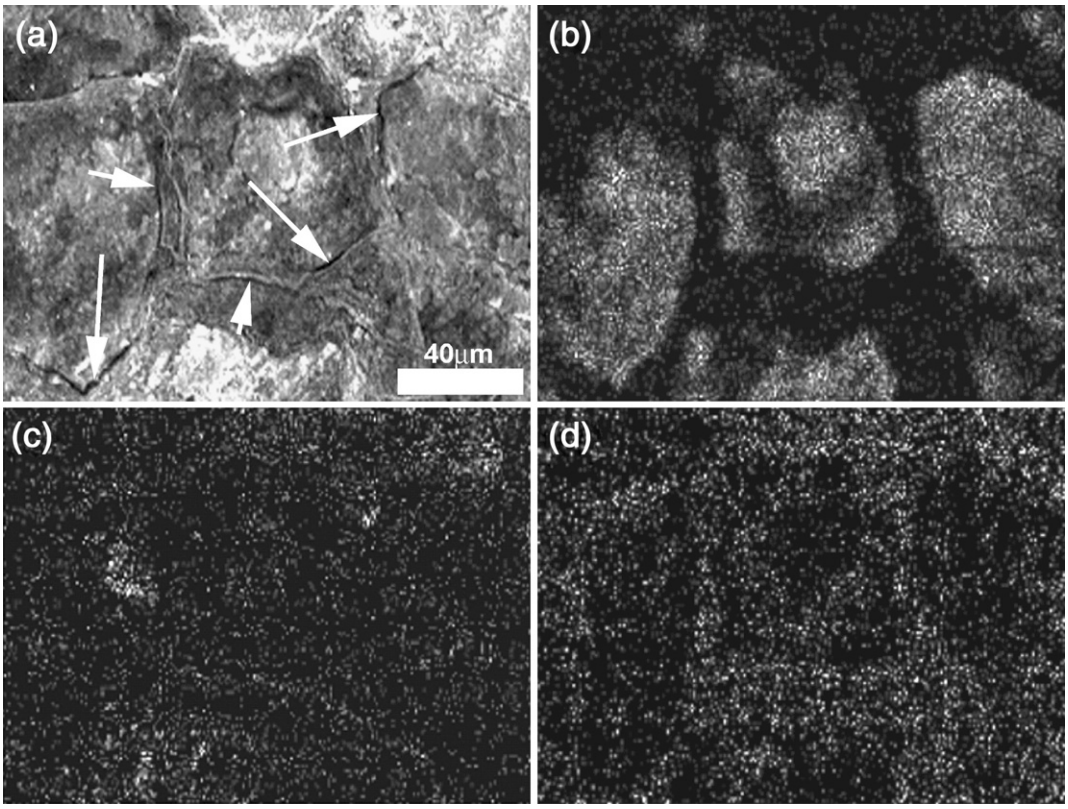

Fig. 8. SEM surface image of electrode with TiC_P/Ni coating after 400 welds (a) showing cracking at coating-sealed Zn–Fe interface and corresponding EDX element maps of Ti K_α (b), Fe K_α (c) and Zn K_α (d).

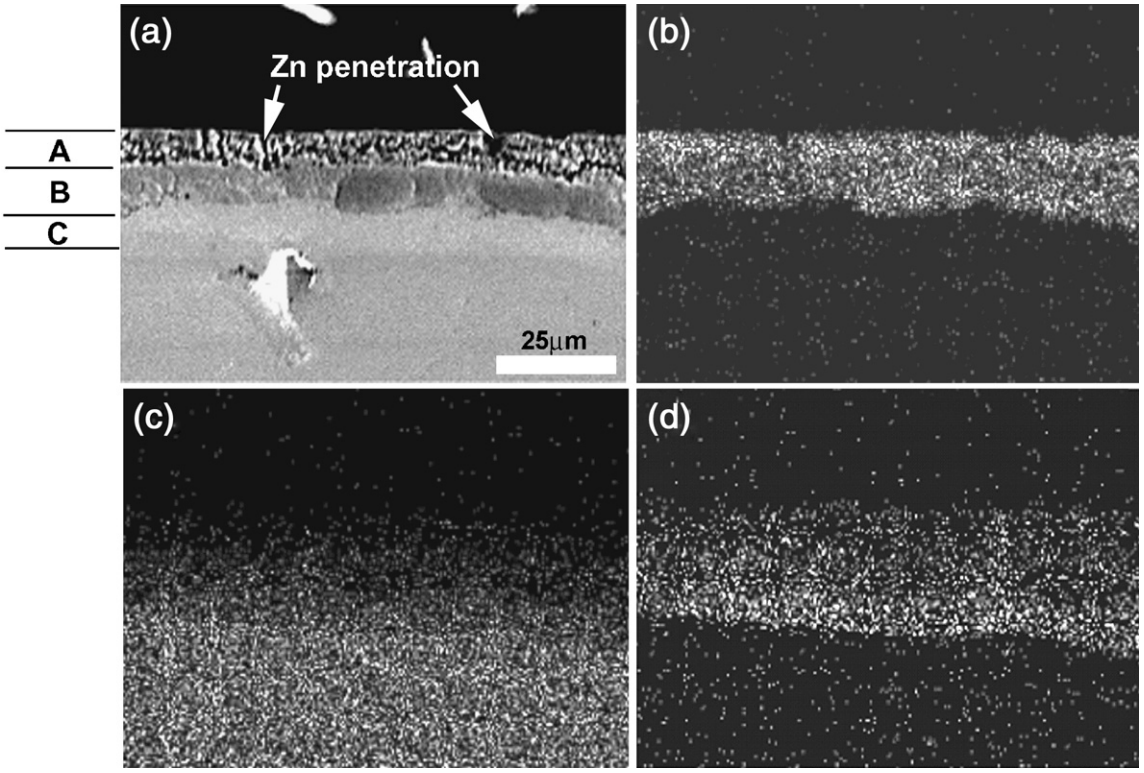

Fig. 9. SEM cross-section of electrode with TiC_P/Ni coating after 100 welds (a) showing granular and loose layer (A), dense layer (B) and Cu–Zn alloy layer (C) and EDX element maps of Ti K_α (b), Cu K_α (c) and Zn K_α (d).

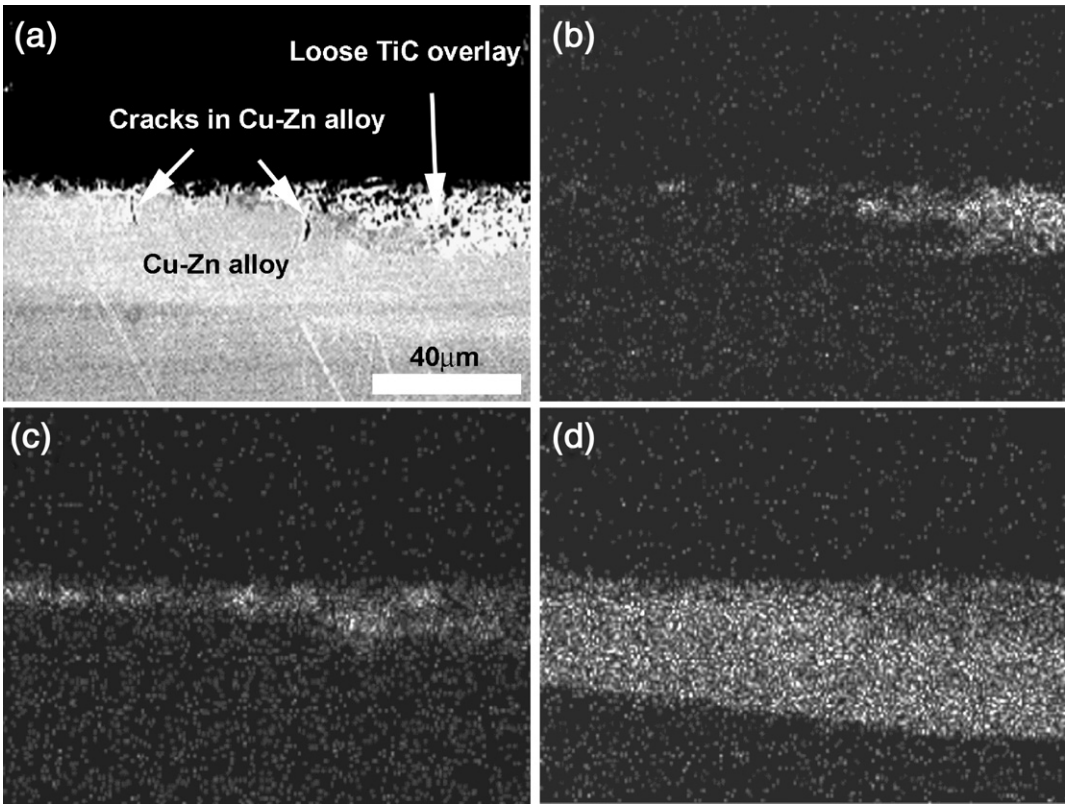

Fig. 10. SEM cross-section of electrode with TiC_P/Ni coating after 400 welds (a) and EDX element maps of Ti K_α (b), Fe K_α (c) and Zn K_α (d).

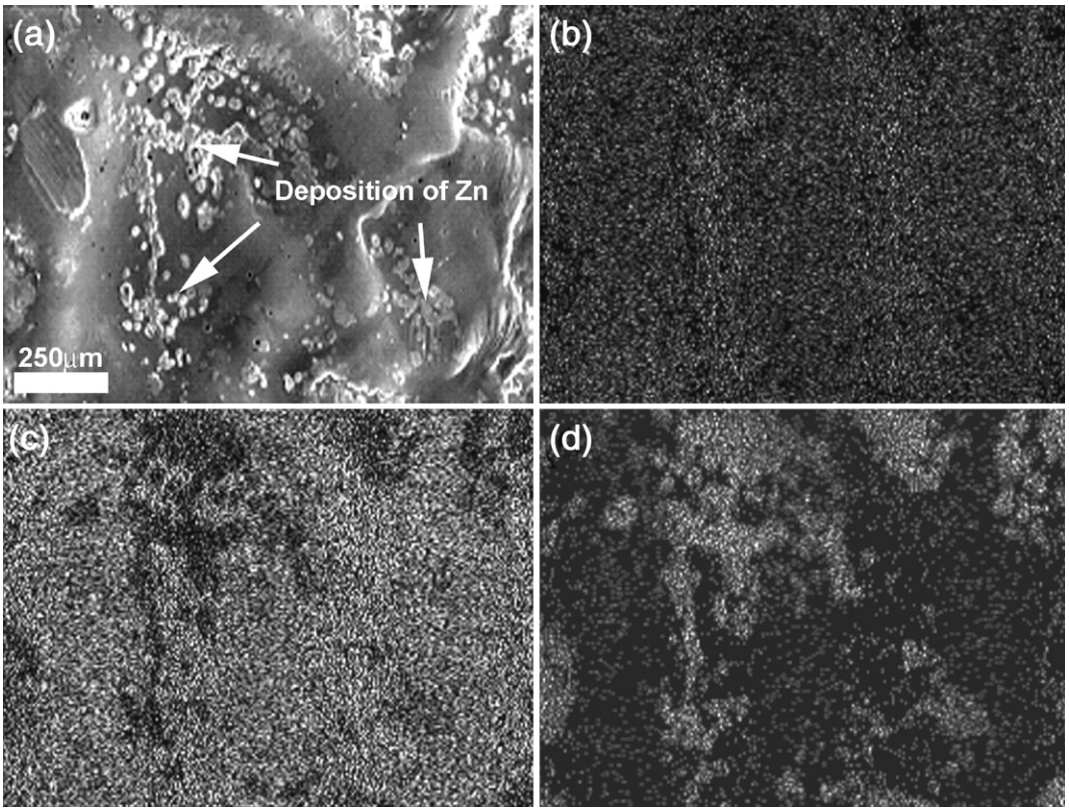

Fig. 11. SEM surface image of electrode with multi-layer Ni/(TiC_P/Ni)/Ni coatings after 1 weld (a) and EDX element maps of Ti K_α (b), Ni K_α (c) and Zn K_α (d).

to 100 welds (Fig. 12). In addition, similar to the monolithic TiC_P/Ni coating, molten Zn containing Fe penetrated into the coating through the newly formed cracks (Fig. 12). It is worth noticing that a large percentage of Ni/(TiC_P/Ni) coating still covered the electrode surface and the diameter of newly formed islands between cracks was relatively large (150–200 μm) compared to that of the TiC_P/Ni coating at 100 welds (Fig. 7). When welding to 400 welds, it was found that the diameter of islands decreased to 100–180 μm and width of cracks also increased, revealing continuous cracking of Ni/(TiC_P/Ni)/Ni coating during welding. However, the Ni/(TiC_P/Ni)/Ni coating still remained on the surface even after it cracked.

Fig. 13 shows the cross-section of an electrode with Ni/(TiC_P/Ni)/Ni coating after 100 welds. Except for rarely observed cracking within the coating, the coating was dense and adhered to the substrate. Zn was mainly present on the coating surface and did not show much diffusion into the substrate to form Cu–Zn alloy. Consistent with surface observation, SEM cross-section of electrode with Ni/(TiC_P/Ni)/Ni coating after 400 welds demonstrated that the coating started to develop cracking (Fig. 14). In addition, delamination at coating–substrate interface was also visible (Fig. 14). As a result, Zn was found to penetrate and diffuse into the coating mainly through the cracks and delamination. However, different from the monolithic TiC_P/Ni coating, the multi-layer Ni/(TiC_P/Ni)/Ni coating did not exhibit the granular and loose structure up to 400 welds and showed only limited cracking and delamination. Particularly, Zn seemed to have more difficulty to diffuse through the Ni layer than TiC_P/Ni coating. Consequently, no visible Cu–Zn alloy layer could be found. Table 2 summarizes the difference in metallurgical behaviours of monolithic TiC_P/Ni coating and multi-layer Ni/(TiC_P/Ni)/Ni coating before and after certain numbers of welds and clearly shows the benefits of multi-Ni/(TiC_P/Ni)/Ni coating in preventing the coating from cracking and the substrate from alloying with Zn.

EDX analyses were used to determine the amount of coating materials remaining on the surface of the electrodes and the amount of electrode materials including coating and copper substrate removal to the sheet. As shown in Table 3, consistent with the XRD and SEM results, although the TiC_P/Ni coating had much higher TiC content than the multi-layer Ni/(TiC_P/Ni)/Ni coating prior to welding, it showed a much faster loss rate during welding due to the formation of a granular loose coating which is easily pulled off by adhesion to the workpiece.

4. Discussion

It is well known that resistance spot welding electrodes must possess (1) high electrical conductivity to minimize electrode heating; (2) high thermal conductivity to dissipate heat from the contact area between the electrode and the worksheet; (3) high hot strength to resist deformation caused by the application of high welding forces; and (4) ability to provide resistance to alloying. As a part of the electrode material after deposition, the composite coatings have the advantages of (3) and (4) mentioned above, especially acting as barrier layer between molten Zn and copper alloy substrate to arrest formation of Cu–Zn alloy [12]. This benefit of composite coating is similar to the

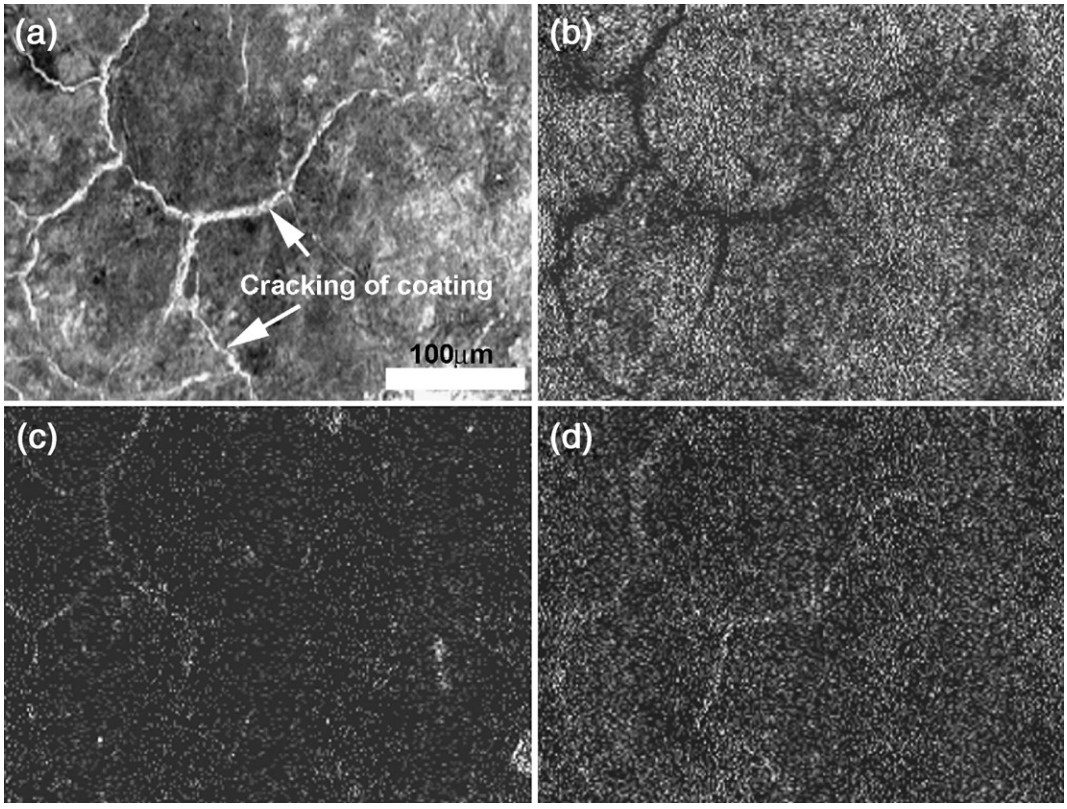

Fig. 12. SEM surface image of electrode with multi-layer Ni/(TiC_P/Ni)/Ni coatings after 100 welds (a) and EDX element maps of Ti K_α (b), Fe K_α (c) and Zn K_α (d).

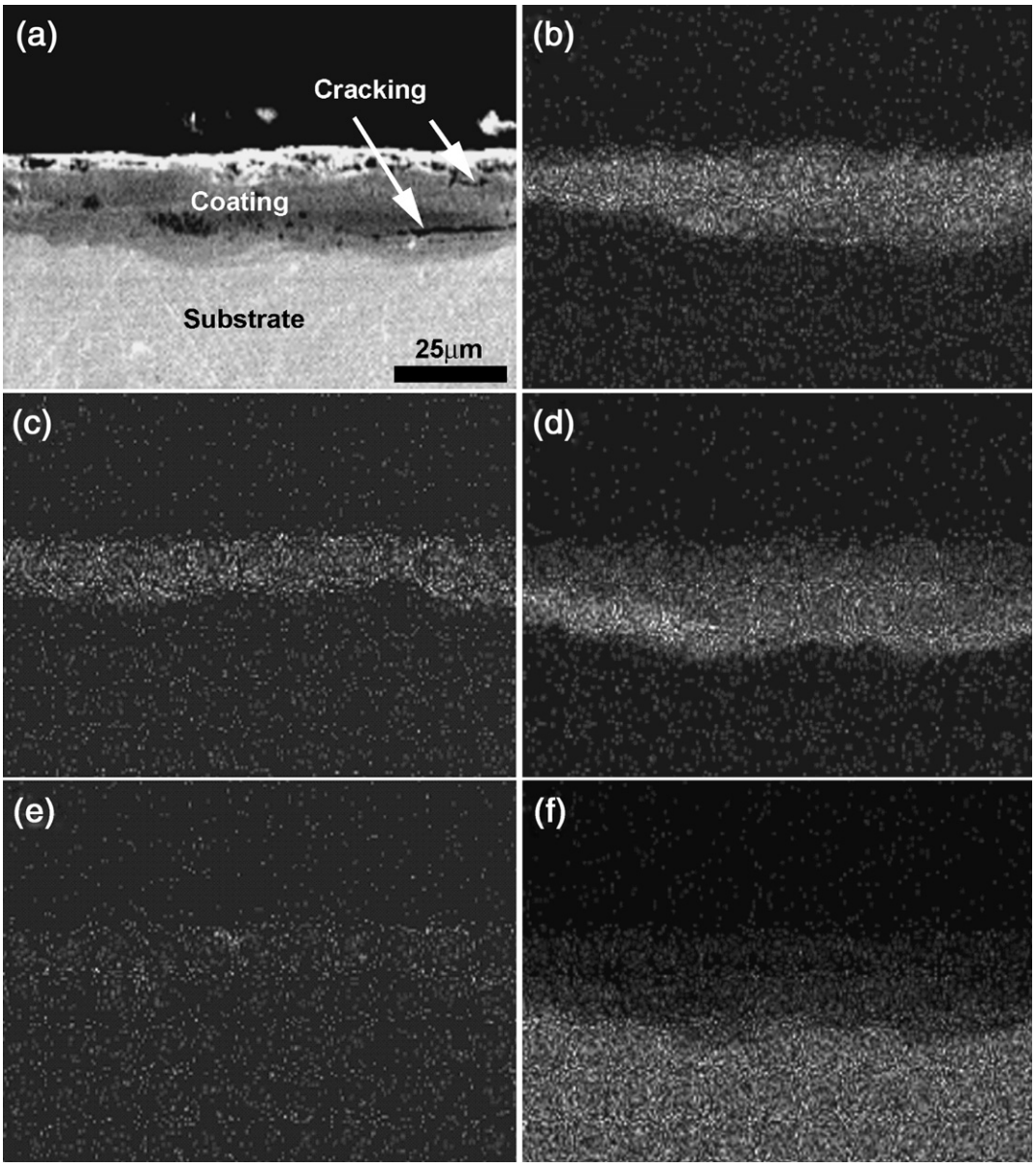

Fig. 13. SEM cross-section of electrode with multi-layer Ni/(TiC_P/Ni)/Ni coatings after 100 welds (a) and EDX element maps of Ti K_α (b), Zn K_α (c), Ni K_α (d), Fe K_α (e) and Cu K_α (f).

formation of Al_2O_3 layer on the top surface of an aluminum oxide dispersion strengthened copper, which prevents the Cu–Zn alloy layer from spalling and suppresses the deposition of Zn–Fe on the electrode face and hence alloying between Zn and copper [14].

However, there are many cracks within as-deposited monolithic TiC_P/Ni coatings and delamination at coating–substrate interface. Consequently, molten Zn penetrates into the coating via those defects (Fig. 5) and local removal of TiC_P/Ni coating due to sticking especially at delamination regions is also found from the first weld (Fig. 4). Continued welding causes further alloying between copper and penetrated Zn (layer "C" in Fig. 9) as well as cracking of the coating, resulting in the formation of surface granular layer (layer "A" in Fig. 9) that was then removed due to surface sticking (Fig. 10). It is thought that penetration of molten Zn has two different effects on coated electrodes. On one hand, a negative effect is accelerated formation of a Cu–Zn alloy layer underneath the coating, starting from very early stages of welding, which may accelerate degradation of electrodes during their use. On the other hand, as a positive effect, solidification of penetrated molten Zn (Fe) brazes the cracked TiC_P/Ni coating together and helps adhesion of the coating to the substrate, which helps keep the coating on the surface to protect the Cu–Zn alloy from being lost to the sheet. As a result of these effects, electrodes with TiC_P/Ni coating show a fast tip growth up to 100 welds due to fast loss of the coating; whereas a slow tip growth process occurs after 100 welds due to increased difficulty of loss of Zn-brazed coating (Fig. 1). A secondary effect is also possible due to reduced current density due to the growth of contact diameter and hence less heat generation. More importantly, however, the granular microstructure formed on the outer surface of the TiC_P/

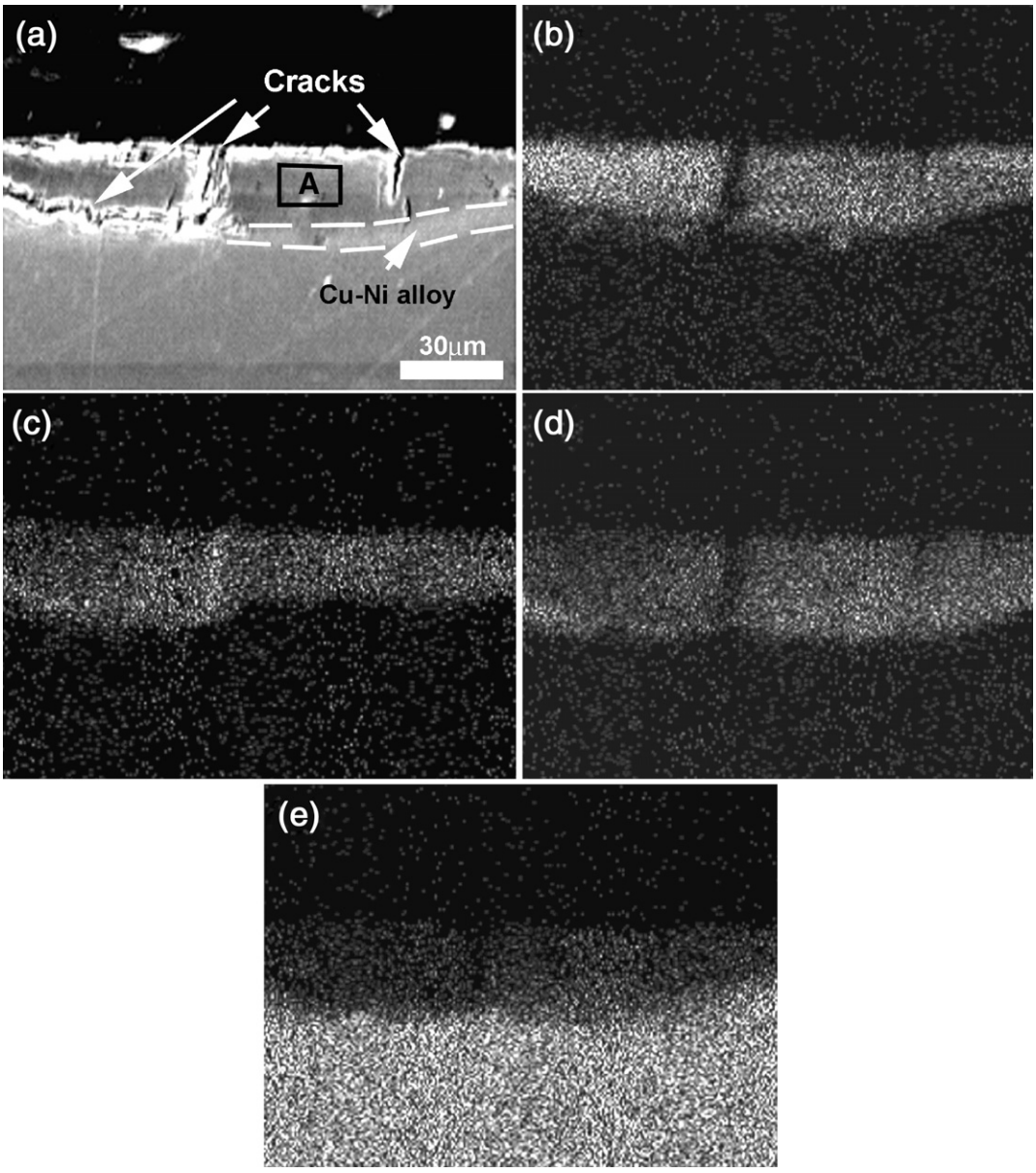

Fig. 14. SEM cross-section of electrode with multi-layer Ni/(TiC_P/Ni)/Ni coatings after 400 welds (a) and EDX element maps of Ti K_α (b), Zn K_α (c), Ni K_α (d) and Cu K_α (e).

Ni coating (Fig. 9), which might be caused by significant cracking of the coating due to thermal and impact fatigue, causes loss of the key feature of a dense coating as a barrier layer. Consequently, when sticking occurs, the granular TiC_P/Ni coating will be easily removed to the worksheet surface. In addition, cracks are again formed at the TiC_P/Ni coating-solidified Zn interface during continued welding probably due to continual mechanical and thermal impact on the electrode surface (Fig. 8). Progressive granulation and removal of the TiC_P/Ni coating eventually results in almost all the coating being lost onto the worksheet surfaces. At this stage, the coated electrode behaves like an uncoated electrode.

Table 2
Summary of different metallurgical behaviors of TiC_P/Ni coating and Ni/(TiC_P/Ni)/Ni coatings after certain numbers of welds

Coatings		Diameter of islands (μm)	Depth of Zn penetration and diffusion (μm)	Cu–Zn alloy layer (μm)	Density of coating
TiC_P/Ni coating	As-coated	250			Dense
	100 welds	50–80	25–35	12	Granular
	400 welds	30–60	28–45	30	Granular
Ni/(TiC_P/Ni)/Ni coatings	As-coated	None			Dense
	100 welds	150–200	10–15	Little	Dense
	400 welds	100–180	15–24	Little	Dense

The hardness of the as-deposited TiC_P/Ni coating is about HV 1000. In general, the harder the composite, the lower the toughness. As a result, many cracks form within the as-deposited TiC_P/Ni coating due to its low toughness and operational stress during deposition [13]. In addition, during welding, the TiC_P/Ni coating further cracks upon mechanical and thermal impact, and eventually develops a fractured

Table 3
Composition of electrodes and sheet surface after certain numbers of welds, as determined by EDX (wt.%)

Eelectrode	Welds	Tip surface composition					Sheet surface			
		Ti	Ni	Cu	Zn	Fe	Ti	Cu	Zn	Ni
TiC_P/Ni coating	0	48.52	20.53	24.79						
	1	42.64	17.27	17.68	12.98	1.03	1.28	7.11	29.83	
	10	35.48	10.42	14.28	32.01	2.41	0.41	2.73	34.58	
	100	24.93	0.90	13.28	36.00	11.14	0.36	6.48	45.93	
	400	2.00					0.21	5.64	46.81	
Ni/(TiC_P/Ni)Ni coating	0	15.35	68.07	13.93						
	1	10.69	56.74		28.97	1.51	0.29	0	30.39	5.86
	10	8.67	37.10	6.58	42.14	1.59	0	0	44.80	0.75
	100	18.97	7.00	10.78	43.73	8.03	0.29	4.25	47.9	2.31
	400	9.11	1.49	9.04	55.68	12.19	0	6.93	57.24	0

granular microstructure. Such significantly cracked and granular TiC_P/Ni coating is no longer able to act as a barrier layer to prevent Zn from penetration and alloying with copper.

On the contrary, the multi-layer Ni/(TiC_P/Ni)/Ni coating contains more Ni than monolithic TiC_P/Ni and, hence, shows a medium hardness around HV 500 [13]. As discussed in Part I of this work [13], increasing the Ni content, which is a metal with high ductility and toughness acting as an excellent binder for TiC composite, would increase the toughness of the overall Ni/(TiC_P/Ni)/Ni coating. As a result, a crack-free and continuous Ni/(TiC_P/Ni)/Ni coating was obtained [13]. Consequently, upon welding, Ni/(TiC_P/Ni)/Ni coating provided a better barrier action than the TiC_P/Ni coating, especially before 100 welds (Figs. 12 and 13): with the dense Ni/(TiC_P/Ni)/Ni coating maintained on the substrate surface, no formation of Cu–Zn alloy layer was possible. However, continuing to weld after 100 welds eventually resulted in diffusion and penetration of Zn into the Ni/(TiC_P/Ni)/Ni coating. The composition (wt.%) of the central Ni/(TiC_P/Ni)/Ni coating region at 400 welds (indicated by area A in Fig. 14) was determined by EDX to be 25.5Ti–29.7Ni–30.6Zn–12.9Cu. According to the Ni–Zn and Cu–Zn phase diagrams, some Zn might have reacted with Ni and/or Cu during the welding process to form Ni–Zn, Cu–Zn or Ni–Cu–Zn compounds, for example, NiZn (β phase) [15]. Such compound phases were not detected in XRD probably due to their low content below the detection limit of the XRD diffractometer (Fig. 3). The formation of brittle intermetallic compounds would decrease the toughness of the Ni/(TiC_P/Ni)/Ni coating and, hence, would cause cracking of the coating after 100 welds (Figs. 12 and 13). However, much fewer cracks formed within the Ni/(TiC_P/Ni)/Ni coating compared to the TiC_P/Ni coating, and no granulation of the coating occurred up to 400 welds, demonstrating the better functioning of the former coating as a barrier to delay the formation of Cu–Zn alloy layers. It appears that the toughness of the coating is more critical than its hardness. A dense coating with relatively high toughness may have the ability to reduce or avoid cracking of the coating during welding and hence acts as a good barrier layer for a longer period.

From a different viewpoint, Tanaka reported a relatively long electrode life when resistance-welding Zn–Ni-coated sheet comparing to Zn-coated sheet, owing to disturbance of the formation of Zn–Cu–Fe alloy at the tip surface, thus delaying diffusion of Zn in the electrode [9]. Such beneficial influence of addition of Ni into a plated layer may also be significant when the coating contains high Ni content, such as the multi-layer Ni/(TiC_P/Ni)/Ni coating, showing no visible formation of Cu–Zn alloy and much slower diffusion of Zn into the coating (Fig. 14).

It has been shown that material loss from electrodes (i.e., pitting or erosion) is one of the primary reasons leading to the growth of electrode tips. As a result, electrodes with multi-layer Ni/(TiC_P/Ni)/Ni composite coating demonstrated slower tip diameter growth rate than electrodes coated with monolithic TiC_P/Ni owing to its dense and less cracked state as-deposited and, hence, much lower removal to the work sheets (Fig. 1).

5. Conclusions

(1) Molten Zn penetrated into the monolithic TiC_P/Ni coating via the cracks that were present within the as-deposited coating even from first weld.
(2) The monolithic TiC_P/Ni coating continued to crack during welding due to action of the welding force and its low toughness, resulting in the formation of a granular broken structure near the outer surface that was easily removed by worksheet adhesion and the formation of Cu–Zn alloy layers underneath the coating.
(3) The multi-layer Ni/TiC–Ni/Ni coating showed much less cracking and, hence, formed a better barrier against Zn penetration and reaction with the copper electrodes.
(4) With a multi-layer Ni/(TiC_P/Ni)/Ni coating on the electrode surface, pitting (erosion) of electrode was remarkably reduced, and hence, a slower growth rate of tip diameter was observed.

References

[1] P. Howe, S.C. Kelly, A comparison of the resistance spot weldability of bare, hot-dipped, galvannealed, and electrogalvanized DQSK sheet steels, International Congress and Exposition, Detroit Michigan, February 29–March 4, 1988.
[2] J.D. Parker, N.T. Williams, R.J. Holiday, Science and Technology of Welding and Joining 3 (1998) 65.
[3] R. Holiday, J.D. Parker, N.T. Williams, Welding in the World 37 (1996) 186.
[4] R. Holliday, J.D. Parker, N.T. Williams, Welding in the World 35 (1995) 160.

[5] R. Ikeda, K. Yasuda, K. Hashiguchi, T. Okita, T. Yahaba, Effect of Electrode Configuration on Electrode Life in Resistance Spot Welding of Galvannealed Steel and Aluminum Alloy For Car Body Sheets, IBEC 1995, Advanced Technologies and Proceedings, 1995, p. 144.
[6] T. Saito, Y. Takahashi, T. Nishi, Nippon Steel Technical Report 37 (1998) 24.
[7] L.M. Friedman, R.B. McCauley, Welding Journal (1969 Oct) 454.
[8] Y. Tanaka, M. Sakaguchi, H. Shirasawa, M. Miyahara, S. Normura, International Journal of Materials and Product Technology 2 (1987) 64.
[9] C.T. Lane, C.D. Sorensen, G.B. Hunter, S.A. Gedeon, T.W. Eagar, Welding Journal (1987 Sep) 260.
[10] R. Holliday, J.D. Parker, N.T. Williams, Key Engineering Materials 99–100 (1995) 95.
[11] S.J. Dong, Y. Zhou, Metall. Mater. Trans., A Phys. Metall. Mater. Sci. 34 (2003) 1501.
[12] Zheng Chen, N. Scotchmer, Y. Zhou, Surface Modification of Resistance Welding Electrodes by Electro-Spark Deposited Coatings, Materials Science and Technology MS&T 2005, Pittsburgh, USA, 2005.
[13] Z. Chen, Y. Zhou, Surf. Coat. Technol. (in press).
[14] M. Kumagai, K. Nagata, Spot Weldability of Aluminum Oxide Dispersion Strengthened Copper Electrodes for Alternate Welding of Mild Steel Sheets and Galvanised Steel Sheets, Sumitomo Light Metals Technical Report vol. 31 (1990) 18.
[15] N.-Y. Tang, X. Su, M. Touri, Calphad 25 (2001) 267.